Journal of Materials Chemistry A

PAPER

View Article Online
View Journal | View Issue

Cite this: J. Mater. Chem. A, 2015, 3, 6373

Unusual photophysical properties of conjugated, alternating indigo–fluorene copolymers†

João Pina,*[a] J. Sérgio Seixas de Melo,[a] Anika Eckert[b] and Ullrich Scherf[b]

Received 18th November 2014
Accepted 26th January 2015

DOI: 10.1039/c4ta06272h

www.rsc.org/MaterialsA

Alternating indigo–fluorene copolymers have been synthesized by the coupling of didromoindigo and fluorendiboronic ester monomers. The low solubility of the copolymers only allowed for the synthesis of moderate molecular weight copolymers, with a degree of polymerization (DP) up to 11. The syntheses were accomplished through a 10% excess of the fluorene-based monomer component in an AA/BB-type polycondensation mixture. Next, a comprehensive spectroscopic (singlet–singlet and transient – from fs to μs – absorption, fluorescence and phosphorescence spectra) and photophysical investigation (fluorescence, phosphorescence and triplet lifetimes together with fluorescence and triplet occupation and singlet oxygen sensitization quantum yields) of the copolymers was carried out. The experiments were complemented with the spectroscopic results from a fluorene–indigo–fluorene model compound, as well as by TDDFT calculations. Based on our kinetics analysis, singlet energy transfer from the fluorene to indigo moieties is found to be inefficient. Besides the low energy indigo-related absorption band, an additional intermediate energy absorption band is also observed between 400 nm and 500 nm, both for the copolymer and for the model compound. Excitation into this band causes an emission of the indigo moiety. The triplet state is found to be mainly localized at the fluorene moiety; however, the decrease of the phosphorescence quantum yield (ϕ_{Ph}) when going from the monomeric 9,9-bis(dodecyl)fluorene (0.075) to the model trimer (0.003) and copolymer (ϕ_{Ph} = 0.008) suggests that excitation energy transfer occurs in the triplet state. This is further confirmed by the higher level of delocalization of the transient triplet–triplet absorption spectra of the copolymer relative to the monomeric 9,9-bis(dodecyl)fluorene.

Introduction

Over the past decade, organic photovoltaic devices based on π-delocalized conjugated polymers have attracted considerable interest from academy and industry, owing to their potential as an economically viable solar energy harvesting medium by virtue of their ability to provide good solution processability, and as lightweight and flexible substrates, together with reduced environmental impact.[1–5] For optimum cell performance, broad-absorption and narrow band-gap polymers are highly desirable, as they are more efficient in capturing solar energy.[6] In general, narrow band-gap polymers can be constructed by combining an electron-rich donor (D) and an electron-deficient acceptor (A) repeat units into alternating donor–acceptor (DA) copolymers.[7–10] Such conjugated DA copolymers offer the opportunity for tuning the band-gaps and HOMO/LUMO energy levels, through varying the donor and acceptor strengths and π-electron topology.[2,11] So far, devices based on polymer/fullerene bulk heterojunctions as the active layer exhibit the highest reported power conversion efficiencies (PCEs).[12–16] Despite the great potential of organic solar cells, their limited PCE and environmental stability have to date been the major obstacles to the large-scale commercialization of organic photovoltaic devices. Driving organic photovoltaics (OPV) forward onto commercial products still requires further developments to be made in donor and acceptor materials, including improving their high throughput processing. Regarding the electron-donating (copolymer) component of the active bulk heterojunction blend, one promising strategy is to incorporate high performance synthetic dye units as the electron-poor building blocks of DA copolymers, such as diketopyrrolopyrrole (DPP), isoindigo, benzodipyrrolidone (BDP) and benzodifuranones.[17–22] Also indigo as a "natural" dye unit has been incorporated into the backbone of such DA copolymers.[23–25] In the present study, we report the synthesis of an alternating indigo–fluorene copolymer in a Suzuki-type polycondensation of didromoindigo and fluorendiboronic ester monomers, followed by a detailed study of its spectroscopic and photophysical properties, including its energy transfer behavior. In comparison to previous work by Yamamoto and co-

[a]Coimbra Chemistry Centre, Department of Chemistry, University of Coimbra, Rua Larga, 3004-535 Coimbra, Portugal. E-mail: jpina@qui.uc.pt

[b]Makromolekulare Chemie, Bergische Universität Wuppertal, Gaußtraße 20, 42097 Wuppertal, Germany

† Electronic supplementary information (ESI) available. See DOI: 10.1039/c4ta06272h

workers,[25] the longer alkyl side chains of our copolymers led to an improved solubility and enabled a higher degree of polymerization. Copolymers with such dye-based building blocks often show broad and strong absorption in the UV-Vis and NIR regions, indicating a good match of their absorption profile with the solar emission spectrum.[25–30] Indigo and its derivatives are long been known and used for their bright and brilliant color, as well as their high photochemical stability.[31]

Today, indigo-based dyes have found new purpose in the flourishing field of organic electronics research.[17,32] This revival is driven by the need for materials that combine favorable optical and charge transport properties with solution processability and high stability, particularly for OPV applications.

Isoindigo-based low band-gap copolymers have shown high power conversion efficiencies in bulk heterojunction-type OPV devices of up to 6.3%.[22] However, for the corresponding indigo-based copolymers, high performing OPV devices have not been reported, until now. The motivation for our investigations was to contribute to the first detailed study of the photophysical properties of an indigo-based alternating, conjugated copolymer. One of the challenges when dealing with indigo-based DA copolymers is their poor solubility. Structural modification of the indigo amide groups can lead to indigo derivatives with improved solubility, thus allowing solution processing into thin films.[26,33] However, in our first study we used non-substituted indigo moieties, since *N*-substitution alters the photophysical properties of indigo-based materials. Transferring our results to *N*-substituted indigo building blocks will be the focus of forthcoming investigations.

Experimental section

Absorption and fluorescence spectra were recorded on a Cary 5000 UV-Vis-NIR and a Horiba-Jobin-Yvon Fluorog 3-22 spectrometer, respectively. Phosphorescence measurements were made in glasses at 77 K and used the Horiba-Jobin-Ivon Fluorog 3-22 spectrometer, equipped with a 1934 D phosphorimeter unit.

The fluorescence quantum yields were measured using cresyl violet perchlorate ($\phi_F = 0.54$)[34,35] in methanol solution as the standard, while the phosphorescence quantum yields were determined using benzophenone ($\phi_{Ph} = 0.84$)[36] in ethanol solution as the standard.

Fluorescence decays were measured using a home-built picosecond time-correlated single-photon counting (TCSPC) apparatus described elsewhere in the literature.[37] The fluorescence decays and the instrumental response function (IRF) were collected using a timescale of 1024 (or 4096) channels, up to a maximum of 5×10^3 were reached. Deconvolution of the fluorescence decay curves was performed using the modulating function method, as implemented by G. Striker in the SAND program, as previously reported in the literature.[38]

The ground state molecular geometry was optimized using the density functional theory (DFT) by means of the Gaussian 03 program, under B3LYP/6-31G** level.[39–41] Optimal geometries were determined on isolated entities in a vacuum and no conformation restrictions were imposed. For the resulting optimized geometries, time-dependent DFT calculations (TD-DFT), using the same functional and basis set as those in the previously calculations, were performed to predict the vertical electronic excitation energies. The molecular orbital contours were plotted using GaussView 5.0.

The experimental setup used to obtain the triplet spectra and the triplet yields is described elsewhere in the literature.[42] First-order kinetics was observed for the decay of the lowest triplet state.

Room temperature singlet oxygen phosphorescence was detected at 1270 nm using a Hamamatsu R5509-42 photomultiplier, cooled to 193 K in a liquid nitrogen chamber (products for research model PC176TSCE-005), following laser excitation of the aerated solutions at 355 nm with an adapted Applied Photophysics flash kinetic spectrometer, as reported elsewhere in the literature.[43] 1*H*-Phenalen-1-one (perinaphthenone) in toluene ($\lambda_{exc} = 355$ nm), $\phi_\Delta = 0.93$, was used as the standard.[44]

The experimental setup for the ultrafast spectroscopic and kinetics measurements consisted of a broadband (350–1600 nm) HELIOS pump-probe femtosecond transient absorption spectrometer from Ultrafast Systems, equipped with an amplified femtosecond Spectra-Physics Solstice-100F laser (displaying a pulse width of 128 fs and 1 kHz repetition rate), coupled with a Spectra-Physics TOPAS Prime F optical parametric amplifier (195–22 000 nm) for pulse pump generation. The probe light in the UV range was generated by passing a small portion of the 795 nm light from the Solstice-100F laser through a computerized optical delay (with a time window of up to 8 ns) and then focusing in a vertical translating CaF_2 crystal to generate a white-light continuum (350–750 nm). All the measurements were obtained in a 2 mm quartz cuvette, with absorptions in the range 1.0–1.8 at the pump excitation wavelength. To avoid photodegradation, the solutions were stirred during the experiments or kept in movement using a motorized translating sample holder. The transient absorption data were analyzed using the Surface Xplorer PRO program from Ultrafast Systems.

The NMR spectra were recorded on Bruker Advance 400 or Advance III 600 NMR spectrometers. MALDI-TOF mass spectra were recorded on a Bruker Reflex TOF. The GPC measurements were carried out in tetrahydrofuran solution on a PSS/Agilent SECurity GPC system with UV-Vis and RI detection by using PSS SDV analytical linear M columns (pre-column: 8 × 50 mm, pore size 5 μm; followed by two columns: 8 × 300 mm, pore size 5 μm). For calibration, narrowly distributed polystyrene standards were applied.

Synthesis and characterization

In this study, (*E*)-6,6′-dibromo-[2,2′-biindolinylidene]-3,3′-dione (6,6-dibromoindigo) was used as the starting material for the synthesis of the model (trimer) compound and the copolymers, following a literature procedure described elsewhere.[45]

Synthesis of (*E*)-6,6′-bis(9,9-didodecylfluoren-2-yl)-[2,2′-biindolinylidene]-3,3′-dione (6,6-di(fluorene-2-yl)indigo). A mixture of 1.0 g (2.38 mmol) of (*E*)-6,6′-dibromo-[2,2′-biindolinylidene]-3,3′-dione (6,6-dibromoindigo), 3.14 g (5.0 mmol) of 2-(9,9-

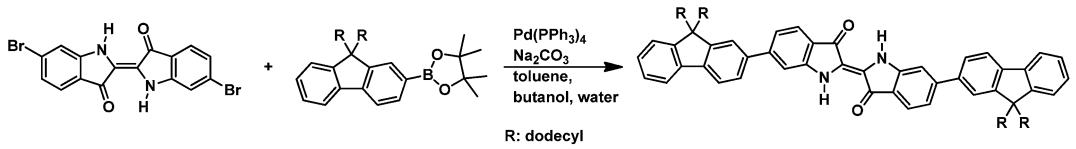

didodecylfluoren-2-yl)-4,4,5,5-tetramethyl-1,3,2-dioxaborolane, and 0.33 g (3.09 mmol) of sodium carbonate was dissolved in 10 mL of water/50 mL of *n*-butanol under inert conditions. Next, 0.14 g (0.12 mmol) of tetrakis(triphenylphosphane)palladium(0) dissolved in toluene was added to this solution. After 12 h stirring at 120 °C, the dark green solution was diluted with chloroform. The organic layer was washed with dilute aqueous hydrochloric acid, aqueous sodium hydrogen carbonate solution, aqueous EDTA solution, and aqueous sodium chloride solution. Purification by multiple silica column chromatography with hexane/dichloromethane gave the trimer as a dark green solid (yield: 451 mg, 15%).

^{1}H-NMR (400 MHz, C_2D_6SO, 300 K): δ [ppm] = 8.97 (bs, 2H), 7.76–7.71 (m, 4H), 7.68–7.76 (m, 2H), 7.57–7.54 (m, 4H), 7.32–7.25 (m, 10H), 1.95–1.92 (m, 8H), 1.32–0.99 (m, 72H), 0.82–0.74 (m, 12H), 0.66–0.56 (m, 8H).

A ^{13}C NMR spectrum could not be recorded due to the limited solubility.

MS (MALDI-TOF): $[C_{90}H_{122}N_2O_2]^+$ m/z = 1262.6

Synthesis of poly{(*E*)-6-(9,9-didodecylfluoren-2-yl)-6′-[2,2′-biindolinylidene]-3,3′-dione} (alternating indole–fluorene copolymer).

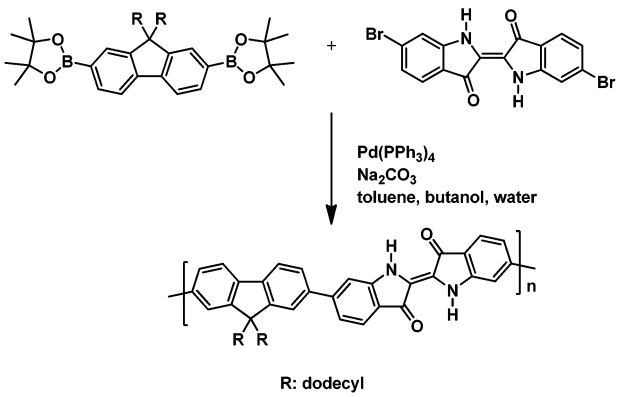

Under an argon atmosphere, 1.98 g (2.62 mmol) of 2,2′-(9,9-didodecylfluoren-2,7-diyl)bis(4,4,5,5-tetramethyl-1,3,2-dioxaborolane), 1.0 g of (2.38 mmol) (*E*)-6,6′-dibromo-[2,2′-biindolinylidene]-3,3′-dione, and 0.34 g (3.17 mmol) of sodium carbonate were dissolved in the two-phase solvent mixture composed of 70 mL of butanol, 24 mL of water, and 50 mL of toluene. Next, a solution of 0.14 g (0.12 mmol) of tetrakis-(triphenylphosphane)palladium(0) in toluene was added. The solution was stirred for 72 h at 120 °C. The resulting dark green mixture was diluted with chloroform and the organic phase washed with dilute aqueous hydrochloric acid, aqueous sodium hydrogen carbonate solution, aqueous EDTA solution, and aqueous sodium chloride solution. Following, the polymer solution was treated overnight with a solution of sodium diethyldithiocarbamate in water to remove catalyst traces. The copolymer solution was concentrated and precipitated into methanol. The raw copolymer was purified by Soxhlet extraction with methanol, acetone, ethyl acetate, dichloromethane, and chloroform, leaving the higher molecular weight material as a chloroform-insoluble residue. The highest molecular weight soluble dichloromethane (DCM) and chloroform fractions of the target copolymer were isolated as dark green powders (yields: DCM fraction: 247 mg, 13%; chloroform fraction: 81 mg, 4%).

GPC: (DCM fraction, solvent: THF): M_n [g mol^{-1}] = 5000; M_w = 6000; PDI = 1.21.

GPC: ($CHCl_3$ fraction, solvent: THF): M_n [g mol^{-1}] = 7200; M_w = 8900; PDI = 1.23.

^{1}H-NMR (400 MHz, $C_2D_2Cl_4$, 353 K): δ [ppm] = 9.02 (bs, 2H), 7.77–7.59 (m, 8H), 7.40–7.12 (m, 4H), 2.23–1.84 (m, 4H), 1.24–1.08 (m, 36H), 0.82–0.80 (m, 10H).

A ^{13}C NMR spectrum could not be recorded due to the limited solubility.

Results and discussion

Synthesis

The alternating indigo–fluorene copolymer was synthesized in a Suzuki-type aryl–aryl cross-coupling of 6,6′-dibromoindigo and 2,2′-(9,9-didodecylfluoren-2,7-diyl)-bis(4,4,5,5-tetramethyl-1,3,2-dioxaborolane) with $Pd(PPh_3)_4$ as the catalyst and sodium carbonate as the base in a two-phase solvent mixture of toluene/water/*n*-butanol. Hereby, the fluorene component was used in 10% excess, in order to limit the chain length of the products and to circumvent problems with the low solubility of the resulting copolymer. The mixture was stirred for 72 h at 120 °C. The organic phase, after aqueous workup, was dried, concentrated, and precipitated into methanol. Subsequent solvent extraction gave two copolymer fractions of moderate molecular weight with M_n 5000 and 7200, and DP of 8 and 11, respectively (the molecular weight data are presented in Table 1). The obtained degrees of polymerization mirror the 1.1 : 1 monomer stoichiometry that was used by us. The fluorene–indigo–fluorene model compound was synthesized in a Suzuki-type coupling of 6,6′-dibromoindigo and 2-(9,9-didodecylfluoren-2-yl)-4,4,5,5-tetramethyl-1,3,2-dioxaborolane under similar reaction conditions (reaction time 24 h, purification by column chromatography). The chemical structures of the investigated

Table 1 Molecular weight data (M_n, M_w, PD) of the two investigated indigo–fluorene copolymer fractions

Copolymer	M_n (g mol^{-1})	M_w (g mol^{-1})	PD
$n = 8$	5000	6000	1.21
$n = 11$	7200	8900	1.23

materials are depicted in Scheme 1. In addition and for comparison, also "monomeric" 9,9-bis(dodecyl)fluorene and indigo were also investigated.

Spectroscopic properties

Singlet-state. Fig. 1 presents the absorption spectra of the two copolymer fractions and the fluorene–indigo–fluorene model oligomer, together with those of the isolated "monomeric" units 9,9-bis(dodecyl)fluorene and indigo, all in dioxane solution. The absorption spectra of the oligomeric and polymeric indigo–fluorene derivatives display the characteristic absorption features of the monomeric units (although red-shifted, especially for the high-energy, fluorene-related bands), together with an additional "in-between" band with an absorption maximum at 410–431 nm (see Fig. 1 and Table 2). Upon going from the trimeric model compound to the indigo–fluorene copolymer, negligible red-shifts for the low- and high-energy absorption bands are observed, whereas the "in-between" absorption band displays a more pronounced red-shift of ~21 nm (Fig. 1 and Table 2). The absorption behavior, first, indicates a lower energy excitation that is localized to the indigo (H-chromophore) without an extended π-conjugated character. The "in-between" absorption band is assigned to a charge-transfer transition; for this, please see the following discussion.

The fluorescence emission spectra of the copolymers and the fluorene–indigo–fluorene model oligomer collected at several excitation wavelengths are depicted in Fig. 2. Except for some difference in the shape and peak position of the high-energy emission band at 350–450 nm, and in agreement to what was

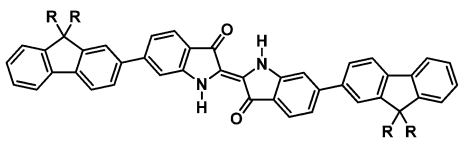

Fluorene-Indigo-Fluorene Trimer

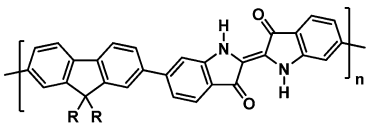

Alternating Indigo-Fluorene Copolymer
(R: dodecyl; n=8 or n=11)

Scheme 1 Chemical structures of the alternating indigo–fluorene copolymer and the 6,6′-di(fluorene-2-yl)indigo model (trimer) compound.

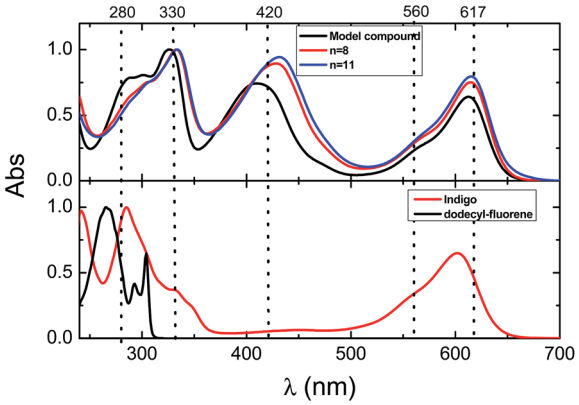

Fig. 1 Normalized absorption spectra for the investigated alternating indigo–fluorene copolymers and the fluorene–indigo–fluorene model compound (top), as well as 9,9-bis(dodecyl)fluorene and indigo (bottom), all in dioxane solution at room temperature. The vertical dashed lines are set at the position of the long wavelength absorption maximum of the copolymer and at four other wavelengths and are guidelines to the eyes.

found in the absorption spectra, no changes were seen in the emission features when going from the model oligomer to the copolymers with $n = 8$ and 11 (Fig. 2 and Table 2). The fluorescence maxima of the low-energy emission band is found to be at a constant position at 645 nm, both for the copolymer and for the fluorene–indigo–fluorene model compound, and also for (monomeric) indigo, while a ~20 nm red-shift is seen for the position of the high-energy emission maxima. The constancy observed in the spectral features of the low-energy emission band shows that this band corresponds to strongly localized chromophoric (indigo) units. When excited into the high-energy, fluorene-related absorption band, the emission spectra of the copolymer and model fluorene–indigo–fluorene compound display characteristic emission features of fluorene (peaking at 374–394 nm) and indigo (645 nm) moieties, see Table 2 and Fig. S1 in the ESI.† However, since for the fluorene–indigo copolymers direct excitation of the indigo moiety is always possible (see indigo's absorption spectrum, Fig. 1), it is impossible, based only on the emission spectra (with excitation at 280/330 nm), to conclude on the occurrence of an intramolecular energy transfer from the fluorene to indigo units.

Further photophysical parameters, including quantum yields (fluorescence, ϕ_F, and phosphorescence, ϕ_{Ph}) and the corresponding lifetimes obtained in dioxane or methylcyclohexane solutions (τ_F, τ_{Ph} and τ_T), are presented in Table 2. No significant changes (within experimental error) are found in the ϕ_F values (in the 0.009–0.011 range) for the copolymers or model compound when excited into the absorption band of the indigo moiety ($\lambda_{exc} = 560$ nm).

Both for the model compound and the copolymer fractions, the fluorescence decays were both collected in the emission band related to the 9,9-bis(dodecyl)fluorene ($\lambda_{em} = 395$ nm) and indigo unit ($\lambda_{em} = 650$ nm) with excitation at 285 nm and 391 nm, respectively (Fig. 3), using a ps-TCSPC equipment (~3 ps time resolution), see the Experimental section for further details. The decays collected in the indigo emission band were

Table 2 Spectroscopic (absorption, fluorescence and phosphorescence emission and triplet absorption maxima) and photophysical data (including fluorescence, ϕ_F, and phosphorescence, ϕ_{Ph}, quantum yields and lifetimes, τ_F, τ_{Ph} and τ_T) for the investigated compounds in dioxane solution (unless stated otherwise)

	λ_{max}^{abs} (nm) 293 K	λ_{max}^{fluo} (nm) 293 K (λ_{exc} = 285 nm)	$\lambda_{max}^{phospha}$ (nm) 77 K	$\lambda_{max}^{T_1 \rightarrow T_n}$ (nm) 293 K	ϕ_F 293 K (λ_{exc} = 560 nm)	τ_F (ns) 293 K	ϕ_{Ph}[a] (77 K)	τ_{Ph}[a] (s) 77 K	ϕ_Δ 293 K	τ_T (μs) 293 K
9,9-Bis(dodecyl)fluorene	265, 293, 304	305, 315	436, 464, 493	375	0.93[e]	5.18	0.075	5.98	—	4.6
Indigo	285, 601	645	—	540[d]	0.0023[b]	0.14[b]	—	—	0.0012[b]	30
Model trimer	326, 410, 612	374, 645	482	555	0.009	0.16[c]	0.003	0.169	0.023	24
Copolymer (n = 8)	333, 428, 615	394, 645	432, 461	630	0.011	0.17[c]	0.008	0.617	0.014	73
Copolymer (n = 11)	333, 431, 615	394, 645	455	610	0.010	0.13[c]	0.008	0.159	0.014	29

[a] Obtained in frozen methylcyclohexane solution (77 K). [b] Data in DMF taken from ref. 46. [c] Fluorescence lifetimes obtained with λ_{exc} = 391 nm and λ_{em} = 650 nm. [d] Obtained by Pulse Radiolysis in benzene solution in the presence of biphenyl or naphthalene as triplet sensitizers.[46] [e] Obtained with excitation at 302 nm and using fluorene in dioxane solution as standard (ϕ_F = 0.68).[36]

found to fit to a mono-exponential decay law, with lifetimes in the 130–170 ps range. The obtained fluorescence decay times are in good agreement with the fluorescence lifetime obtained for indigo in dimethylformamide (DMF)[46] and dioxane,[29,47] see Table 2.

For the investigated copolymers, when the excitation/emission was performed/collected in the spectral region related to the fluorene moiety, the decays could be fitted with a mono-exponential decay law (Fig. 3). However, for the model fluorene–indigo–fluorene oligomer, in agreement to what was previously found for poly[9,9-bis(2-ethylhexyl)fluorene] (*i.e.*, PF2/6), two decay times were necessary for the fitting. This behavior should be associated to an initial, instantaneously formed (non-relaxed) species (120 ps), which is then further transformed into a relaxed species (1.3 ns).[48] In the case of the alternating indigo–fluorene copolymers, the decay times (in the 1.13–1.30 ns range) are higher than those found for the long-lived component in PF2/6. Moreover and interesting to note, the increased decay time obtained for the fluorene-related emission (relaxed state) remained constant (1.13 ns) upon increasing the copolymer length (going from n = 8 to 11). This observation, together with the absence of any rising component when collecting the decays in the indigo-related spectral region (see the single exponential decay of Fig. 3B), indicates that the singlet energy transfer between the fluorene and indigo moieties is an inefficient, neglectable process. However, the fact that the isolated 9,9-bis(dodecyl)fluorene monomer exhibits a much extended decay time of 5 ns (see Fig. S2 in ESI†) documents that both the copolymer (for n = 8 and 11) and model fluorene–indigo–fluorene compound show some degree of delocalization/electronic communication between the neighboring fluorene and indigo units.

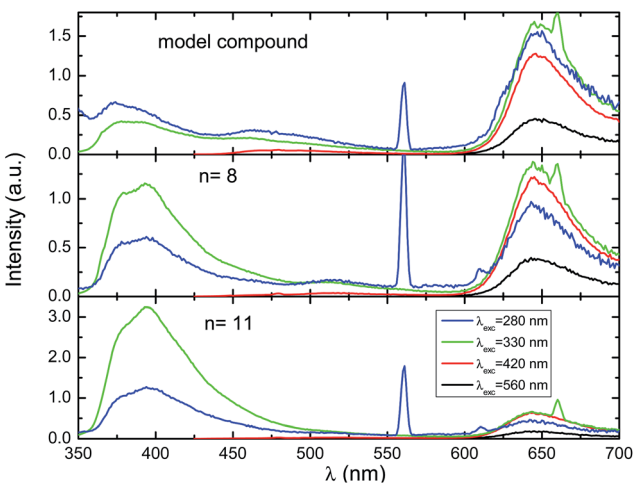

Fig. 2 Fluorescence emission spectra for the copolymers and model compound collected at different excitation wavelengths in dioxane solution at T = 293 K. The peaks at 560 nm and 660 nm in the blue and green spectra, respectively, result from the frequency doubling of the excitation wavelengths (280 nm and 330 nm).

Triplet-state. In contrast to indigo and indigo derivatives, where no phosphorescence emission is observed, fluorene derivatives and oligo/polyfluorenes are known to show phosphorescence.[36,46,49] In order to investigate the phosphorescence properties of the mixed indigo–fluorene systems, phosphorescence emission spectra were recorded and phosphorescence quantum yields estimated for the model oligomer and copolymers in frozen methylcyclohexane solution (77 K), see Fig. 4 and Table 2 (the spectrum for 9,9-bis(dodecyl)fluorene is added for comparison). Quite similar phosphorescence emission spectra were found for 9,9-bis(dodecyl)fluorene, the model oligomer, and the two copolymers under investigation. Herein, the spectrum of the higher molecular weight copolymer (n = 11) did not show, in contrast to the other spectra, any vibronic resolution. In summary, the phosphorescence data clearly indicate that the phosphorescence of these compounds originates from the localized fluorene moieties.

Nevertheless, the decrease of the phosphorescence yield from 0.075 (for 9,9-bis(dodecyl)fluorene) to 0.003 (model fluorene–indigo–fluorene compound and indigo–fluorene copolymers (ϕ_{Ph} = 0.008)) indicates that some energy transfer should occur in the triplet state. Herein, the assumed absence of phosphorescence for the indigo moiety is not a contraindication against energy transfer in the triplet state manifold. Indeed, the significant decrease in the phosphorescence lifetime τ_{Ph} values when going from 9,9-bis(dodecyl)fluorene (5.98 s) or fluorene (5.5 s)[36] to the investigated indigo–fluorene

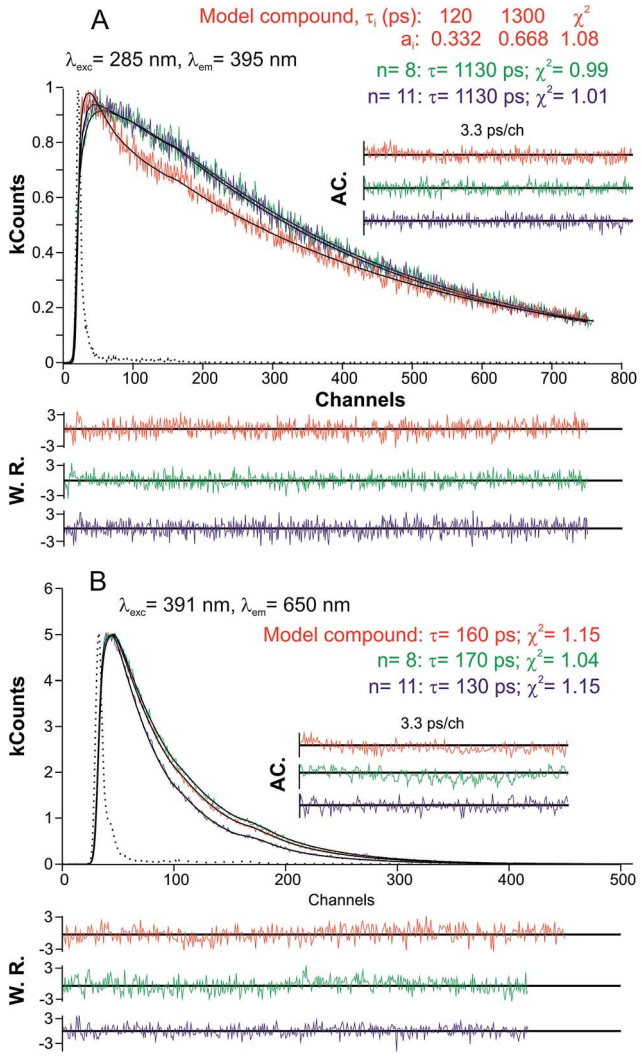

Fig. 3 Room temperature fluorescence emission decays for the investigated fluorene–indigo–fluorene model compound and the two copolymer fractions (with $n = 8$ and 11 repeat units, respectively) obtained with (A) $\lambda_{exc} = 285$ nm and collected at $\lambda_{em} = 395$ nm and (B) $\lambda_{exc} = 391$ nm and $\lambda_{em} = 650$ nm in dioxane solution. For a better judgment of the quality of the fits, the weighted residuals (W.R.), autocorrelation functions (AC.), and χ^2 values are also presented. The dashed line in the decays is the instrumental response function.

compounds (τ_{Ph} values in the 0.159–0.617 s range) clearly implies the presence of an energy transfer in the triplet state.

Fig. 5 presents the transient triplet–triplet absorption spectra obtained upon laser flash photolysis at 355 nm of degassed dioxane (oxygen free) solution for the copolymers and the model compound in comparison to 9,9-bis(dodecyl)fluorene (excitation at 266 nm). For the copolymers and the trimeric model compound, broad transient absorption bands in the 400–700 nm region were found. The transient triplet–triplet absorption spectra and triplet lifetimes (τ_T in the 24–73 μs range) of the investigated compounds are in good agreement with the data obtained in pulse radiolysis experiments for indigo in benzene solution (transient absorption in the 450–700 nm region and $\tau_T = 30$ μs),[46,50] thus supporting the occurrence

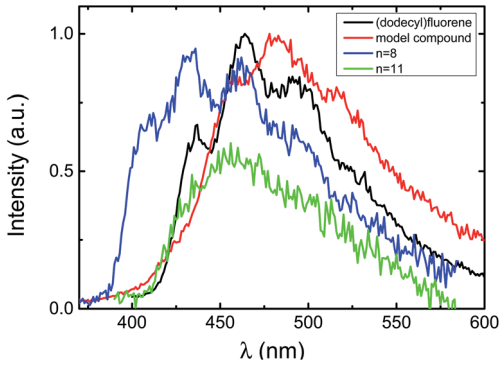

Fig. 4 Normalized phosphorescence emission spectra for the investigated compounds in methylcyclohexane at $T = 77$ K.

of electronic interactions between the fluorene and indigo units in the triplet state.

Singlet oxygen can be detected by its characteristic phosphorescence following triplet energy transfer. The singlet oxygen quantum yields obtained for the investigated compounds (trimer, copolymers) are in the 0.014–0.023 range, thus one order of magnitude higher than the value found for indigo in DMF solution, $\phi_\Delta = 0.0012$ (Table 2). Considering that, in general, the singlet oxygen quantum yields cannot be higher than the quantum yield of triplet formation ($\phi_\Delta \leq \phi_T$), the low ϕ_Δ values found for the investigated compounds show that, in agreement with the behavior found for indigo, the nonradiative, internal conversion decay channel is the dominating excited state deactivation process.[32,46]

Femtosecond transient absorption

Finally, Fig. 6 shows the transient absorption spectra and the associated decay kinetics for the investigated compounds in aerated dioxane solutions at room temperature from pump-probe femtosecond time-resolved transient absorption spectroscopy. The compounds were excited at 325 nm (pump light), thus promoting the population of the excited state, followed by an analysis/probing with light in the 340–750 nm range and

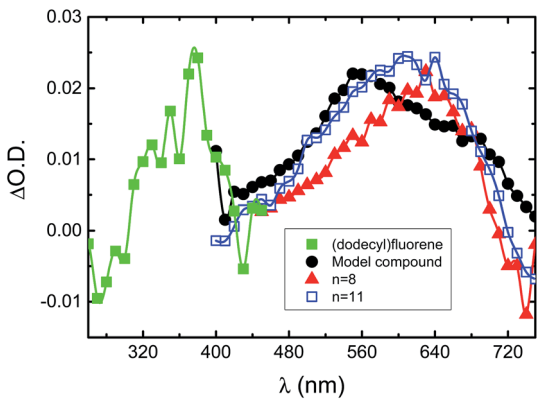

Fig. 5 Normalized transient singlet–triplet difference absorption spectra for the investigated compounds in dioxane solution at $T = 293$ K.

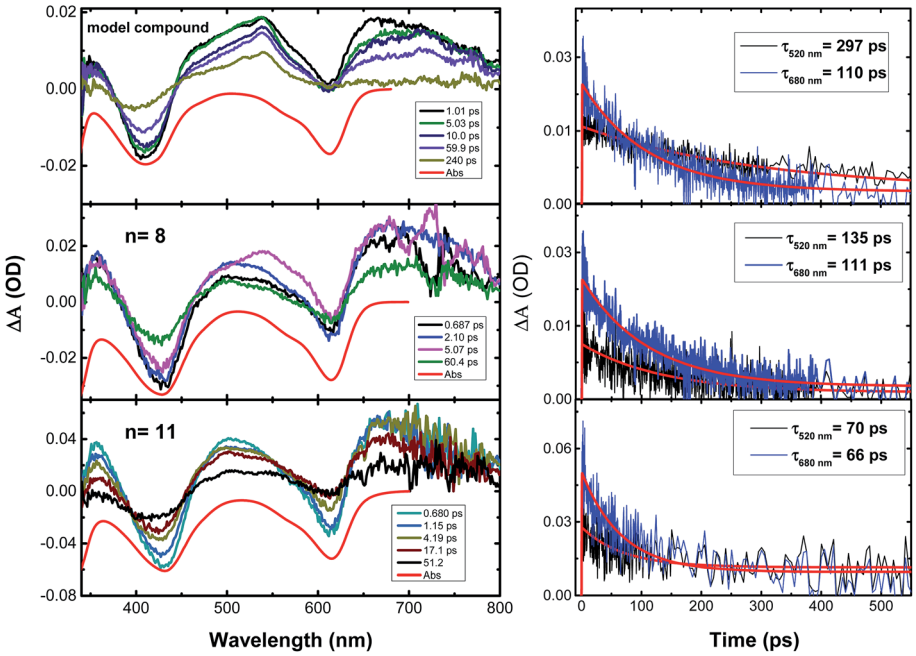

Fig. 6 Femtosecond transient absorption difference spectra collected at different time delays following excitation at 325 nm along with the transient absorption decays collected at 520 and 680 nm in dioxane solution (for the model trimer and copolymers with $n = 8$ and 11, respectively). For comparison, the ground state absorption spectra are also presented (red lines, as spectra of reverse sign).

recording the evolution of the transient absorption spectra and decay kinetics within a 7 ns time-window. Broad transient absorption bands were found, with the positive signals ($\Delta A/A > 0$) corresponding to excited state absorption features, while the negative signals were attributed to the ground state bleaching (Fig. 6). The transient absorption spectra of 9,9-bis(dodecyl) fluorene and indigo in dioxane solution were also recorded, for comparison. When exciting in the lowest energy 0–0 absorption band ($\lambda_{exc} = 303$ nm) of 9,9-bis(dodecyl)fluorene, no signals were observed that could be attributed to the excited state absorption of the monomeric fluorene. However, indigo itself (under excitation at $\lambda_{exc} = 285$ and 325 nm) displayed a broad transient absorption band in the 350–750 nm range (see Fig. S3 in ESI†), similar to the observations for the oligomeric model compound and copolymers.

For the model oligomer and copolymers, kinetic traces were analyzed at 520 nm and 680 nm. The decays could be fitted mono-exponentially with decay times in the range of 66–297 ps (see Fig. 6). This finding, especially the absence of an additional short decay time associated with energy transfer,[51] together with the absence of a femtosecond transient absorption response for 9,9-bis(dodecyl)fluorene, indicates that the excited state absorption of the indigo–fluorene compounds originates from the indigo moiety.

Theoretical calculations

To gain further insights in to the electronic structure of the investigated compounds, DFT calculations were performed to determine the optimized ground state geometry, together with the molecular orbital distribution for the fluorene–indigo–fluorene (trimeric) model compound (Fig. 7). To reduce the computational time, the 9,9-bis(dodecyl)-substituents of the fluorene unit were replaced by methyl groups. Additionally, the vibrational frequencies were also computed in order to verify the absence of imaginary frequencies, thus documenting that the optimized geometry really corresponds to a minimum in the potential energy surface. Nevertheless, since no systematic conformational search on the potential energy surface of the molecule was performed, we cannot definitively overlook the existence of other stable conformers as previously described for indigoid dyes with large side groups.[52] The optimized ground state geometry displayed a 35° dihedral angle between the planar indigo cores and terminal fluorene moieties (Fig. 7). This result is in good agreement with the reported values for indigo–bithiophene derivatives, where a dihedral angle of ~24° was found between the indigo and adjacent thiophene units.[23] However, the resulting (moderately) reduced electronic interaction between the fluorene and indigo building blocks alone cannot explain the absence of singlet excited state energy transfer processes. Here, the strong localization of the singlet excited states should play the dominant role.

The vertical excitation transition energies were computed at the B3LYP/6-31G** level by TD-DFT, using the previous optimized geometry as the starting point. The predicted transitions with higher oscillator strength were found at 592 nm ($f = 0.4910$), 494 nm ($f = 0.6413$), and other higher-energy transitions at 333–328 nm ($f = 0.6174$–0.7299). Except for the 494 nm transition, the predicted values are in good agreement with the experimental values (see Table 2). The observed lowest energy transition is characteristic for the π–π^* S_0–S_1 transition of the indigo unit (HOMO → LUMO). The absorption energy is in good agreement with the literature values computed for indigo

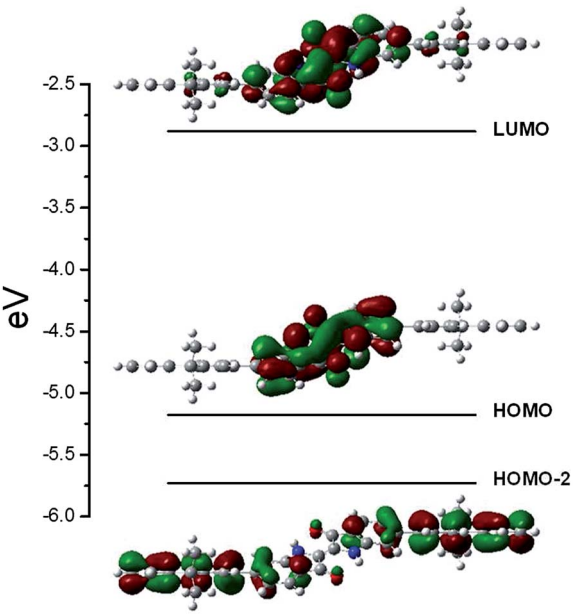

Fig. 7 Ground state optimized geometry at the B3LYP/6-31G** level together with isoenergetic density plots for the HOMO-2, HOMO and LUMO orbitals.

and its derivatives in various solvents using a similar methodology and basis set.[52,53] In agreement with the literature, the HOMO and LUMO levels involved in the transition are completely delocalized over the whole indigo unit, with the HOMO orbital in particular displaying a high degree of electronic conjugation (see Fig. 7).[53]

The computed transition centered at 494 nm is associated with a $S_0 \rightarrow S_3$ transition involving the HOMO-2 and LUMO orbitals, and displays a 84 nm red-shift if compared to the experimental value (410 nm, see Table 2). The molecular orbital contours (Fig. 7) for the HOMO-2 orbital clearly show that the electron density is mainly located in the terminal fluorene substituents, while for the LUMO orbital, the electron density is concentrated in the indigo moiety, thus documenting the intramolecular electron transfer character of this transition. The difference between the predicted (computed in vacuum) and experimental values (measured in dioxane solution) can be interpreted as arising from a dipolar stabilization of the polar charge separated excited-state structure, resulting in a decrease in the computed excitation energy.

An alternative hypothesis for the nature of the additional "in-between" band with an absorption maximum at 410–431 nm for the model compound and copolymers should, however, also be considered. Indeed, similar absorption bands (in the 370–500 nm range) were recently observed for *N*,*N*′-substituted-6,6′-[di-(bi)thienyl]indigo oligomers and copolymers and were attributed to the loss of the H-chromophore nature of indigo (induced by the *N*-substitution with alkyl or acyl groups distorting the planarity of the indigo molecule), leading to the possibility of the formation of *cis*-indigo units and/or the existence of electronically decoupled indole–thiophene chromophores in these derivatives.[23,30] Has previously reported for *N*,*N*′-diacylindigotins, that photoisomerization from the stable *trans*-isomers to the less-stable *cis*-isomers leads to the appearance of a blue-shifted absorption band (with maxima in the 431–477 nm range), when compared to the *trans*-isomers (maxima in the 552–579 nm range).[54] For the *N*,*N*′-substituted-6,6′-[di-thienyl]-indigo derivatives, when excitation was performed in this band, along with the characteristic emission of the indigo H-chromophore with $\lambda_{máx} = 610$ nm, an additional emission band centered at 500 nm was observed, which through the spectral characteristic features of the fluorescence excitation spectra, was attributed to the presence of indole–thiophene conjugation segments.[30]

An additional explanation, also related to the loss of the indigo characteristic H-chromophore, can be found in the reduced form of indigo (leuco form) that, as previously described, also displays an absorption band in a similar region of the spectra (with maxima at ~440 nm).[30,46,55] However, the leuco-indigo form is obtained by treating indigo (or its moiety in the case of copolymers or oligomers where it is a part of the structure) with a strong reducing agent (sodium dithionite) in alkaline media and then stabilizing it in an inert atmosphere. In the present study, the solvent media is not strongly reducing and, therefore, the leuco form, for the investigated derivatives, is absent. Nevertheless, although with our polymers and oligomer this band is present, evidence such as: (i) the absence of substituents on the amide groups of the indigo moieties, together with the fact that it is not likely that in the copolymers a low energy barrier for the *trans–cis* interconversion exists, indicates that the presence of *cis*-indigo units in the copolymers backbones is not likely to be expected; (ii) from the TD–DFT calculations, strong indications are given to the existence of a charge-transfer band between the fluorene and indigo moieties, and (iii) the fluorescence emission spectra obtained with excitation at ~420 nm leading to the characteristic emission of indigo (see Fig. 2), together with (iv) the excitation spectra collected along the indigo emission band displaying the characteristics absorption features of the investigated compounds (Fig. S4 in ESI†), lead us to believe that the nature of this band is better described as originating from a charge-transfer transition. Nevertheless, and as discussed above, the possibility of a partial non-*trans*-indigo conformation cannot be completely discarded and should be considered in forthcoming works.

Conclusions

The synthesis of an alternating, conjugated indigo–fluorene copolymer together with a corresponding fluorene–indigo–fluorene model trimer was accomplished in a Suzuki-type aryl–aryl cross-coupling of 6,6-dibromoindigo and the corresponding 9,9-bis(dodecyl)fluorene di- or monoboronic ester derivatives. The low solubility of the target copolymer only allowed for the generation of moderate molecular weight products with a degree of polymerization of up to 11. The copolymers show a unique electronic behavior, since, in contrast to most conjugated polymers, the red shift with increasing wavelength occurs not for the long wavelength absorption band, but for the next, higher energy absorption band, since the long wavelength band

corresponds to transitions of the electronically localized indigo chromophores. The absorption spectra of the model oligomer and copolymers displayed fluorene- and indigo-related absorption features, together with a charge-transfer band at an intermediate absorption energy. Theoretical (DFT) calculations on the oligomeric model compound support this interpretation of the experimental results. The intermediate energy excitation was assigned to a HOMO-2 → LUMO transition, with a charge transfer character involving both the fluorene (as the electron donor) and indigo units (as the electron acceptor). Furthermore, possible energy transfer processes in the singlet and triplet state were investigated. Singlet state excitation energy transfer from the fluorene to indigo unit seems to be an inoperative process, as the singlet excited states are highly localized. However, phosphorescence and transient absorption data support the occurrence of increased electronic interaction between the fluorene and indigo units in the triplet state.

As a next step in these studies, the synthesis of true donor–acceptor-type alternating copolymers with on-chain indigo units is planned by replacing the fluorene linkers with electron-rich donor moieties, such as cyclopentadithiophene (CPDT). Hereby, additional substituents in the CPDT unit will help to further improve the solubility of the copolymers.

Acknowledgements

The authors thank the Fundação para a Ciência e Tecnologia (Portugal) and FEDER-COMPETE for financial support through the Coimbra Chemistry Centre (project PEst-OE/QUI/UI0313/2014), Program C2008-DRH05-11-842 (JP). The research leading to these results has received funding from Laserlab-Europe (grant agreement no. 284464, EC's Seventh Framework Programme).

References

1 C. W. Tang, *Appl. Phys. Lett.*, 1986, **48**, 183–185.
2 Z. R. Owczarczyk, W. A. Braunecker, A. Garcia, R. Larsen, A. M. Nardes, N. Kopidakis, D. S. Ginley and D. C. Olson, *Macromolecules*, 2013, **46**, 1350–1360.
3 J. Y. Kim, K. Lee, N. E. Coates, D. Moses, T. Q. Nguyen, M. Dante and A. J. Heeger, *Science*, 2007, **317**, 222–225.
4 C. Li, M. Y. Liu, N. G. Pschirer, M. Baumgarten and K. Mullen, *Chem. Rev.*, 2010, **110**, 6817–6855.
5 T. D. Nielsen, C. Cruickshank, S. Foged, J. Thorsen and F. C. Krebs, *Sol. Energy Mater. Sol. Cells*, 2010, **94**, 1553–1571.
6 C. J. Brabec, *Sol. Energy Mater. Sol. Cells*, 2004, **83**, 273–292.
7 J. Pina, J. Seixas de Melo, R. M. F. Batista, S. P. G. Costa and M. M. M. Raposo, *Phys. Chem. Chem. Phys.*, 2010, **12**, 9719–9725.
8 J. Pina, J. Seixas de Melo, H. D. Burrows, R. M. F. Batista, S. P. G. Costa and M. M. M. Raposo, *J. Phys. Chem. A*, 2007, **111**, 8574–8578.
9 J. Pina, J. S. S. de Melo, R. M. F. Batista, S. P. G. Costa and M. M. M. Raposo, *J. Phys. Chem. B*, 2010, **114**, 4964–4972.
10 J. Pina, J. S. de Melo, D. Breusov and U. Scherf, *Phys. Chem. Chem. Phys.*, 2013, **15**, 15204–15213.
11 Z. Ma, E. Wang, M. E. Jarvid, P. Henriksson, O. Inganas, F. Zhang and M. R. Andersson, *J. Mater. Chem.*, 2012, **22**, 2306–2314.
12 S. H. Park, A. Roy, S. Beaupre, S. Cho, N. Coates, J. S. Moon, D. Moses, M. Leclerc, K. Lee and A. J. Heeger, *Nat. Photonics*, 2009, **3**, 297–302.
13 H.-Y. Chen, J. Hou, S. Zhang, Y. Liang, G. Yang, Y. Yang, L. Yu, Y. Wu and G. Li, *Nat. Photonics*, 2009, **3**, 649–653.
14 G. Dennler, M. C. Scharber and C. J. Brabec, *Adv. Mater.*, 2009, **21**, 1323–1338.
15 Y. Y. Liang, Z. Xu, J. B. Xia, S. T. Tsai, Y. Wu, G. Li, C. Ray and L. P. Yu, *Adv. Mater.*, 2010, **22**, E135–E138.
16 S.-Y. Chang, H.-C. Liao, Y.-T. Shao, Y.-M. Sung, S.-H. Hsu, C.-C. Ho, W.-F. Su and Y.-F. Chen, *J. Mater. Chem. A*, 2013, **1**, 2447–2452.
17 M. J. Robb, S.-Y. Ku, F. G. Brunetti and C. J. Hawker, *J. Polym. Sci., Part A: Polym. Chem.*, 2013, **51**, 1263–1271.
18 K. Cao, Z. Wu, S. Li, B. Sun, G. Zhang and Q. Zhang, *J. Polym. Sci., Part A: Polym. Chem.*, 2013, **51**, 94–100.
19 T. Aysha, S. Luňák Jr, A. Lyčka, J. Vyňuchal, Z. Eliáš, A. Růžička, Z. Padělková and R. Hrdina, *Dyes Pigm.*, 2013, **98**, 530–539.
20 L. Dou, J. You, J. Yang, C.-C. Chen, Y. He, S. Murase, T. Moriarty, K. Emery, G. Li and Y. Yang, *Nat. Photonics*, 2012, **6**, 180–185.
21 J. C. Bijleveld, A. P. Zoombelt, S. G. J. Mathijssen, M. M. Wienk, M. Turbiez, D. M. de Leeuw and R. A. J. Janssen, *J. Am. Chem. Soc.*, 2009, **131**, 16616–16617.
22 E. Wang, Z. Ma, Z. Zhang, K. Vandewal, P. Henriksson, O. Inganäs, F. Zhang and M. R. Andersson, *J. Am. Chem. Soc.*, 2011, **133**, 14244–14247.
23 C. Guo, B. Sun, J. Quinn, Z. Q. Yan and Y. N. Li, *J. Mater. Chem. C*, 2014, **2**, 4289–4296.
24 T. Lei, J. Y. Wang and J. Pei, *Acc. Chem. Res.*, 2014, **47**, 1117–1126.
25 H. Fukumoto, H. Nakajima, T. Kojima and T. Yamamoto, *Materials*, 2014, **7**, 2030–2043.
26 R. Stalder, J. Mei and J. R. Reynolds, *Macromolecules*, 2010, **43**, 8348–8352.
27 B. Liu, Y. Zou, B. Peng, B. Zhao, K. Huang, Y. He and C. Pan, *Polym. Chem.*, 2011, **2**, 1156–1162.
28 M. Yao, M. Araki, H. Senoh, S.-i. Yamazaki, T. Sakai and K. Yasuda, *Chem. Lett.*, 2010, **39**, 950–952.
29 R. Rondao, J. S. de Melo, F. A. Schaberle and G. Voss, *Phys. Chem. Chem. Phys.*, 2012, **14**, 1778–1783.
30 E. D. Glowacki, D. H. Apaydin, Z. Bozkurt, U. Monkowius, K. Demirak, E. Tordin, M. Himmelsbach, C. Schwarzinger, M. Burian, R. T. Lechner, N. Demitri, G. Voss and N. S. Sariciftci, *J. Mater. Chem. C*, 2014, **2**, 8089–8097.
31 M. M. Sousa, C. Miguel, I. Rodrigues, A. J. Parola, F. Pina, J. S. Seixas de Melo and M. J. Melo, *Photochem. Photobiol. Sci.*, 2008, **7**, 1353–1359.
32 E. D. Głowacki, G. Voss and N. S. Sariciftci, *Adv. Mater.*, 2013, **25**, 6783–6800.
33 E. D. Glowacki, G. Voss, K. Demirak, M. Havlicek, N. Sunger, A. C. Okur, U. Monkowius, J. Gasiorowski, L. Leonat and N. S. Sariciftci, *Chem. Commun.*, 2013, **49**, 6063–6065.

34 D. Magde, J. H. Brannon, T. L. Cremers and J. Olmsted, *J. Phys. Chem.*, 1979, **83**, 696–699.
35 J. Olmsted, *J. Phys. Chem.*, 1979, **83**, 2581–2584.
36 M. Montalti, A. Credi, L. Prodi and M. T. Gandolfi, *Handbook of Photochemistry*, CRC Press, Boca Raton, 2006.
37 J. Pina, J. Seixas de Melo, H. D. Burrows, A. L. Maçanita, F. Galbrecht, T. Bunnagel and U. Scherf, *Macromolecules*, 2009, **42**, 1710–1719.
38 G. Striker, V. Subramaniam, C. A. M. Seidel and A. Volkmer, *J. Phys. Chem. B*, 1999, **103**, 8612.
39 M. J. Frisch, G. W. Trucks, H. B. Schlegel, G. E. Scuseria, M. A. Robb, J. R. Cheeseman, J. A. Montgomery, Jr., T. Vreven, K. N. Kudin, J. C. Burant, J. M. Millam, S. S. Iyengar, J. Tomasi, V. Barone, B. Mennucci, M. Cossi, G. Scalmani, N. Rega, G. A. Petersson, H. Nakatsuji, M. Hada, M. Ehara, K. Toyota, R. Fukuda, J. Hasegawa, M. Ishida, T. Nakajima, Y. Honda, O. Kitao, H. Nakai, M. Klene, X. Li, J. E. Knox, H. P. Hratchian, J. B. Cross, V. Bakken, C. Adamo, J. Jaramillo, R. Gomperts, R. E. Stratmann, O. Yazyev, A. J. Austin, R. Cammi, C. Pomelli, J. W. Ochterski, P. Y. Ayala, K. Morokuma, G. A. Voth, P. Salvador, J. J. Dannenberg, V. G. Zakrzewski, S. Dapprich, A. D. Daniels, M. C. Strain, O. Farkas, D. K. Malick, A. D. Rabuck, K. Raghavachari, J. B. Foresman, J. V. Ortiz, Q. Cui, A. G. Baboul, S. Clifford, J. Cioslowski, B. B. Stefanov, G. Liu, A. Liashenko, P. Piskorz, I. Komaromi, R. L. Martin, D. J. Fox, T. Keith, M. A. Al-Laham, C. Y. Peng, A. Nanayakkara, M. Challacombe, P. M. W. Gill, B. Johnson, W. Chen, M. W. Wong, C. Gonzalez and J. A. Pople, Gaussian 03, Revision C.02, Gaussian, Inc., Wallingford CT, 2004.
40 A. D. Becke, *J. Chem. Phys.*, 1993, **98**, 1372–1377.
41 M. M. Francl, W. J. Pietro, W. J. Hehre, J. S. Binkley, M. S. Gordon, D. J. Defrees and J. A. Pople, *J. Chem. Phys.*, 1982, **77**, 3654–3665.
42 J. Pina, H. D. Burrows, R. S. Becker, F. B. Dias, A. L. Maçanita and J. Seixas de Melo, *J. Phys. Chem. B*, 2006, **110**, 6499–6505.
43 J. Pina and J. Seixas de Melo, *Phys. Chem. Chem. Phys.*, 2009, **11**, 8706–8713.
44 C. Flors and S. Nonell, *Helv. Chim. Acta*, 2001, **84**, 2533–2539.
45 J. L. Wolk and A. A. Frimer, *Molecules*, 2010, **15**, 5561–5580.
46 J. Seixas de Melo, A. P. Moura and M. J. Melo, *J. Phys. Chem. A*, 2004, **108**, 6975–6981.
47 J. Seixas de Melo, R. Rondão, H. D. Burrows, M. J. Melo, S. Navaratnam, R. Edge and G. Voss, *Chemphyschem*, 2006, **7**, 2303–2311.
48 J. Pina, J. Seixas de Melo, N. Koenen and U. Scherf, *J. Phys. Chem. B*, 2013, **117**, 7370–7380.
49 A. Monkman, C. Rothe, S. King and F. Dias, in *Polyfluorenes*, ed. U. Scherf and D. Neher, Springer Berlin Heidelberg, 2008, pp. 187–225.
50 J. Seixas de Melo, H. D. Burrows, C. Serpa and L. G. Arnaut, *Angew. Chem., Int. Ed.*, 2007, **46**, 2094–2096.
51 K. Sreenath, C. Yi, K. L. Knappenberger and L. Zhu, *Phys. Chem. Chem. Phys.*, 2014, **16**, 5088–5092.
52 D. Jacquemin, J. Preat, V. Wathelet and E. A. Perpète, *J. Chem. Phys.*, 2006, **124**, 074104.
53 A. Amat, F. Rosi, C. Miliani, A. Sgamellotti and S. Fantacci, *J. Mol. Struct.*, 2011, **993**, 43–51.
54 J.-i. Setsune, H. Wakemoto, T. Matsueda, T. Matsuura, H. Tajima, T. Kitao, S. Ishihara and R. Yamamoto, *J. Chem. Soc., Perkin Trans. 1*, 1984, 2305–2309.
55 R. Rondão, J. Seixas de Melo, M. J. Melo and A. J. Parola, *J. Phys. Chem. A*, 2012, **116**, 2826–2832.

